Bound Water Content and Pore Size Distribution in Swollen Cell Walls Determined by NMR Technology

Xin Gao, Shouzeng Zhuang,* Juwan Jin, and Pingxiang Cao

Nuclear magnetic resonance (NMR) relaxation time distributions can provide detailed information about the moisture in wood. In this paper, the bound water content and pore size distributions in swollen cell wall of two kinds of softwoods (*Pinus sylvestris* and *Cunninghamia lanceolata*) and three kinds of hardwoods (*Populus* sp., *Fraxinus excelsior* L., and *Ochroma lagopus*) were determined by NMR cryoporometry. The total bound water content of swollen cell wall almost exceeds 35%, based on dry mass, which is obviously higher than the fiber saturation point (FSP) (appr. 30%) measured by the extrapolation method. The bound water content of different species is consistent with the hypothesis that with the decrease of basic density, the more bound water could be contained in wood. The proportion of the pore diameter smaller than 1.59 nm is higher than 70%, and the proportion of the pore diameter larger than 4 nm is no more than 10%.

Keywords: Swollen cell wall; Bound water; Nuclear magnetic resonance cryoporometry; T_2 distribution; Pore size distribution; Gibbs-Thomson effect

*Contact information: Faculty of Material Science and Engineering, Nanjing Forestry University, Nanjing 210037, China; *Corresponding author: gaoxin57421@163.com*

INTRODUCTION

Wood is a versatile renewable engineering material that has been widely used in construction and interior decoration. This can be attributed to its superior material properties, such as a favorable mass/strength ratio, easy processing, pleasing optical appearance, and wonderful environmental characteristics. However, it is necessary to improve properties such as dimensional stability, strength, and durability through modification (Wacker 2010; Xie *et al.* 2013). As the proportion of wood harvested from artificial fast-plantation forests is increasing, more and more attention has been paid to wood modification techniques (Hill 2006; Mattos *et al.* 2015).

In the commercial production process, water-soluble polymers such as urea resin, phenolic resin, and polyethylene glycol are commonly used to improve the properties of wood by vacuum-pressure impregnation (Hoffmann 1990; Gindl *et al.* 2003; Jeremic *et al.* 2007; Jeremic and Cooper 2009; Gabrielli and Kamke 2010). It has been widely agreed that only the deposition of polymer (phenolic resin and polyethylene glycol) within the wood cell walls results in improvement of the dimensional stability as well as a high decay resistance. If the polymer is only distributed in the cell lumens, then the modification effect is not obvious (Furuno *et al.* 2004). The effect of preservative treatment also depends on the distribution of the active ingredient of preservative in wood, especially if the agents can penetrate into the cell wall. In recent years, nanoparticles of copper-carbonate and iron oxide in aqueous systems have just begun to be exploited commercially for the preservative treatment of wood, and it is not well

known whether cell walls can be penetrated by nanoparticles (Hiroshi *et al*. 2009). The timber is usually saturated by water-soluble modifying agents through impregnation, and the cell wall is swollen after processing. Therefore, it is necessary to know the pore size distribution within the cell wall corresponding to this particular state (Xie *et al.* 2013).

There are a few experimental methods used to determine the pore size distribution of porous materials. These include the mercury intrusion method, gas adsorption, scanning electron microscope (SEM) analysis, atomic force microscope (AFM) analysis, and gas permeation (Park *et al.* 2006). However, these methods are restricted when applied to measuring the pore diameter distribution of swollen cell walls. First, these methods are generally destructive and invasive, and there is a significant influence on the testing results when they are applied to relatively soft fibrous material. Second, because of the hygroscopic substrate and capillary condensation effect, there is generally a certain content of adsorbed water in porous media. To obtain an accurate pore size distribution, the test specimen must be dried prior to the experiment, thus eliminating the influence of the bound water. However, the porosity of the wood cell wall would significantly change along with the shrinkage of wood during the drying process; therefore, it is difficult to acquire the pore size distribution of swollen cell walls by means of conventional detection methods (Park *et al.* 2006; Zauer *et al.* 2014).

The most commonly employed technique to determine the swollen cell pore size distribution is that of the solute exclusion method, where water-saturated wood is immersed in a solution of probe molecules and allowed to reach equilibrium with the solution (Telkki *et al.* 2013). Probe molecules enter the macropores of the wood (lumens, pits, *etc*.) and if they are small enough, they can also penetrate the cell wall. When probes enter the pores of wood, they replace the water in them, which then dilutes the bulk probe solution remaining outside of the fibers. The decrease in concentration of the probe solution is a measure of the pore volume of the wood. Using probe molecules of different sizes, it is possible to obtain data for the pore size distribution of the wood (Hill 2006; Walker 2006). Most of these studies report a maximum size for swollen cell wall micropores in the region of approximately 2 to 4 nm (Stone and Scallan 1968; Hill 2006; Walker 2006). From the perspective of impregnation, various kinds of spectra and imaging technologies have been used to mark the known-size target particles within cell walls. The research has employed UV (Gindl *et al.* 2003; Gierling *et al.* 2005), X-ray (Smith and Côté 1971, 1972; Furuno *et al.* 2004), Raman (Gierling *et al.* 2005; Jeremic *et al.* 2007), SEM/EDXA (Bolton *et al.* 1988; Wallström and Lindberg 1999), and DSC (Cavallaro *et al.* 2013) measurements. The typical or limiting pore size of swollen cell walls can be estimated by the distribution of probe particles. However, the probe objects penetrate into the cell wall in the manner of diffusion and cannot enter the micropores, which are smaller than the probe objects.

As a superior non-destructive analysis method, nuclear magnetic resonance (NMR) technology has been widely used in porous media research and has made significant progress in studying different solids, such as rock (Westphal *et al.* 2005) and soil (Tian *et al.* 2014). The advantage of NMR is the direct extraction of the relaxation characteristics of fluid (primarily water and oil) in porous media at a certain magnetic field. According to the relaxation time and amplitude of the NMR signals, the size of the pores and the amount of fluid could be determined (Telkki *et al.* 2013).

Based on previous studies, NMR technology has provided an abundance of wood-water relationship information (Maunu 2002). Some research has been carried out using NMR relaxation analysis, including establishing the quantitative relationships between moisture content and free induction decay (FID) signal, providing more detailed information about the different moisture components from T_2 or T_1 relaxation time distributions (Sharp *et al.* 1978; Riggin *et al.* 1979; Menon *et al.* 1987; Araujo *et al.* 1992).

Typically, the distributions of T_2 relaxation time contain a few peaks, from which the components with shorter relaxation times [approximately several milliseconds (ms)] are associated with bound water. The components with longer relaxation times, from dozens of ms to hundreds of ms, are associated with free water, according to the size of lumens (Hartley *et al.* 1994; Labbé *et al.* 2002; Almeida *et al.* 2007; Telkki *et al.* 2013). By comparing the change in relaxation time between modified and unprocessed specimens, the modified effects can also be evaluated (Thygesen and Elder 2008).

NMR is also used as a tool in the investigations of pore size distributions, which method is known as cryporometry (Telkki *et al.* 2013; Kekkonen *et al.* 2014). This method is based on the detection of lowered solid-liquid phase transition temperature of a substance confined to pores. According to the Gibbs-Thomson equation, liquids confined within small pores solidify at a temperature that varies inversely with the pore size. NMR provides a very convenient way of quantifying the amount of liquid within the pores as a function of temperature and subsequently offers a quantitative and non-destructive method for determining pore size distribution (Aksnes and Kimtys 2004). NMR cryoporometry has been used to study various materials including nanomaterials (Hassan 2012; Gouze *et al.* 2014), pulp (Östlund *et al*. 2010), and membranes (Jeon *et al*. 2008). The fiber saturation point and pore size distributions of thermally modified wood were studied by this method (Telkki *et al.* 2013; Kekkonen *et al.* 2014). Thermoporometry is an another method for determination of the pore size distributions based on the same principle, the detection of the melting can be done by sensing the transient heat flows during phase transitions using differential scanning calorimetry (DSC; Zauer *et al.* 2014). Some researchers have used this method to analyze the changes in wood pores after heat treatment (Zauer *et al.* 2014). The influence of the pulping process on the porosity of fibers was also investigated (Park *et al.* 2006).

In this work, the bound water content and pore size distributions of swollen cell walls were determined by NMR cryoporometry. The species with different basic density were selected, because it is considered that with decreasing basic density the cell walls display less resistance to swelling, since the bound water content that corresponds to the fiber point represents a balance between the swelling of cell walls and resistance to the mechanical rigidity (Feist and Tarkow 1967; Walker 2006). Mongolian Scotch Pine (*Pinus sylvestris*), fast-growing poplar (*Populus* sp.), and Chinese fir (*Cunninghamia lanceolata*) were selected as medium density species. A high-density ring porous species of ash (*Fraxinus excelsior* L.), and a low-density species of balsa wood (*Ochroma lagopus*) were also chosen for comparison. The pore size distributions of these commercial species could also provide reference data for the selection of wood chemical modification groups.

EXPERIMENTAL

Materials and Equipment

Pinus sylvestris and *Fraxinus excelsior* L. were felled in Heilongjiang Province, which is located in the northeast region of China. The average basic density of these woods are 0.42 gcm^{-3} and 0.71 gcm^{-3}, respectively. *Cunninghamia lanceolata* was felled in Guangdong Province, and its average basic density is 0.39 gcm^{-3}. *Populus* sp. grew in Dabie Mountain of Anhui Province, and the basic density is 0.44 gcm^{-3}. *Ochroma lagopus* was felled in Xishuangbanna of Yunnan Province, which is located in southwest of China, and its basic density is only 0.16 gcm^{-3}. Discs cut from the fresh trunks were kept in closed, plastic bags in a freezer until sample preparation. Cuboid sample pieces (approximately 6 mm × 6 mm × 20 mm; 20 mm is the longitudinal direction) were cut from the discs. To make the cell wall of the samples fully saturated with water, all the samples were boiled with distilled water before NMR analysis. Meanwhile, the water-soluble resins in the wood, which may have influence on the NMR experiment, could be eliminated.

The NMR experiments were carried out on a 22-MHz MiniMR device that was developed by Niumag Corporation, Shanghai, China. To generate a stable magnetic field, the temperature of the magnetic unit was set to be 32 °C, within a variation of $\pm$0.01 °C. The sample chamber contained a temperature-controlling system range from -40 °C (233K) to 40 °C (313K) with an accuracy of 0.1 °C so that the samples could then be detected at different temperatures.

Theory and Methods

Theory

The moisture content and porosity of porous media could be determined by the analysis of the T_2 relaxation times. As previously mentioned, the NMR signals coming from wood could be associated with solid wood, cell wall bound water, and lumen water. The T_2 signal of solid wood decays rapidly to zero in tens of ms, making it readily separable from the bound water signal, which has a T_2 from about one to a few ms. In contrast, the lumen water has a T_2 ranging from tens to hundreds of ms. The dead time of the NMR device is about 30 μs, which is longer than the relaxation time of solid wood. Hence, it is reasonable to assume that the NMR signal comes only from the liquid water in the samples. The relationship between moisture content and amplitude of NMR signals could then be determined.

The basis to measure pore size distribution using NMR cryoporometry is the melting point depression of a pore-filling substance or adsorbate in small pores, which occurs by osmotic and capillary effects. Because of the increased internal pressure, a depressed melting temperature occurs in the interior of small pores (Aksnes and Kimtys 2004). On the assumption that all pores are cylindrical, the relationship between the pore diameter and the melting point depression was described by the Gibbs-Thomson equation (Park *et al.* 2006; Mario *et al.* 2014). From this equation, it is evident that with decreasing pore diameter, the melting point depression increases.

$$\Delta T_m = T_m - T_m(D) = \frac{4\sigma T_m \cos\theta}{D\Delta H_f \rho} \quad (1)$$

In Eq. 1, T_m is the melting temperature of water, $T_m(D)$ is the melting temperature in the pore (diameter D), σ is the surface tension, θ is the contact angle, and ρ and H_f are the density and specific heat of fusion of water, respectively. It is well known that the melting point of bulk water under ordinary pressure is 0 °C. However, the melting point of liquid would decrease when water locates in micropores, especially if the pores are nanoscale. If the porous media fully saturated with water was frozen with different temperatures, the water in different diameter pores would melt according to the Gibbs-Thomson equation. The T_2 relaxation time of ice amounts only to 6 μs, which is obviously smaller than that of liquid water (milliseconds) (Telkki *et al.* 2013); therefore, the pore size distribution could be determined by the NMR signal changes of different moisture components.

There are two kinds of typical scales for wood porosity: lumens that are micron scale and micropores within cell wall that are nano scale; both of the pores could be considered as cylindrical. The melting point depression of free water in lumens was negligible (Telkki *et al.* 2013) so that the free water could be frozen easily. However, the maximum size for swollen cell wall micropores was in the region of 2 to 4 nm (Stone and Scallan 1968; Walker 2006; Hill 2006; Kekkonen *et al.* 2014). The temperature of water melting in such pores should be lower than -5 °C (Park *et al.* 2006; Mario *et al.* 2014). By suitable selection of temperature, free water in wood could be completely frozen; however, bound water was still liquid as it was in nanoscale pores. According to the relaxation time-distribution of moisture in wood before and after freezing treatment, the total amount of bound water could be determined (Almeida *et al.* 2007; Telkki *et al.* 2013). The sample could be frozen with a series of temperatures and the relaxation time distributions would reflect the solidification of bound water and the pore size distribution of swollen cell wall could be confirmed according to the Gibbs-Thomson equation.

Methods

To determine the pore size distribution within the swollen cell wall, the amount of bound water should be acquired precisely, at first. As mentioned previously, the selection of temperature should confirm that free water in lumens is frozen and bound water is still liquid; the phase transition makes a significant difference in relaxation time distributions. In this experiment, -3 °C (270 K) was chosen as the specific temperature. The reason for this is, according to the Gibbs-Thomson equation, the melting point depression is inversely proportional to the diameter of the pore and the size of lumen is above 10 μm, which corresponds to the maximum melting point depression of 0.004 °C (Telkki *et al.* 2013). The extractives of wood dissolved in water may slightly decrease the melting point, which ranges from 0.1 to 2.0 °C (Walker 2006). In contrast, the largest size of micropores in the cell wall rarely exceeds 4 nm (Hill 2006; Walker 2006), which corresponds to the minimum melting depression of 10 °C (Mario *et al.* 2014).

To calculate the effective pore diameter (D) according to Gibbs-Thomson equation, the following parameters were used: T_m = 273.15 K, σ = 12.1 mJm^{-2}, θ = 180 °, ρ = 10^6 gm^{-3}, and H_f = 333.6 jg^{-1} (Park *et al.* 2006; Simpson and Barton 1991; Zauer *et al.* 2014).

$$D = \frac{k}{\Delta T_m} \approx \frac{39.6nm \cdot K}{\Delta T_m} \quad (2)$$

According to the actual situation of the temperature-controlling system, seven freezing temperatures and the room temperature (24 °C or 297 K) were selected. It is estimated that there exists a nonfreezing layer with a thickness of 0.3 to 0.8 nm, and hence the value of 0.6 nm was added to the NMR cryoporometry diameters in order to obtain the true pore sizes (Kekkonen *et al.* 2014). Comparison of the freezing temperatures and corresponding pore diameters due to the Gibbs-Thomson effect is shown in Table 1.

Table 1. Comparison of the Freezing Temperatures and Corresponding Pore Diameters due to the Gibbs-Thomson Effect

T_m (°C)	D (nm)
-40	1.59
-30	1.92
-20	2.58
-15	3.24
-10	4.66
-5	8.52
-3	13.80

The samples that were inserted in 10-mm OD NMR tubes closed with Teflon caps began with room temperature NMR T_2 scanning. The samples were then frozen, and the T_2 scanning at different temperatures was performed beginning with the lowest temperature. A temperature-controlled refrigerator conditioned the temperatures of samples. To confirm that sample temperatures were uniform, twin samples were prepared, and temperature sensors were placed in them. These samples were placed under the same environment. The temperature change could be used to reflect the status of the samples to be tested. When the size of the samples was small, the set temperature could be achieved by about 10 to 15 min later. The samples were scanned 30 min later than the freezing treatment. Meanwhile, the sample chamber had also been adjusted to the same temperature, which ensured temperature stabilization during the process of the experiment. Analysis of the T_2 relaxation times was performed using the CPMG sequence (Araujo *et al.* 1992; Almeida *et al.* 2007):

$$\{90_x°\text{-}\tau/2\text{-}[180_y°\text{-}\tau\text{-echo-}\tau]_m\} \quad (3)$$

For the present experiments, τ=0.2 ms, the number of echoes according to the sample pieces (softwood was 5000, hardwood was 10,000), echo time was 200 μs, and the relaxation delay and number of accumulated scans were 3s and 16, respectively. Experimental data were processed by Delphi according to the Contin program developed by Provencher (1982a,b).

The moisture content of the samples was determined by the weight difference between the saturated and dried specimens (103±2 °C, 20 h),

$$MC = \frac{m_0 - m_1}{m_1} \cdot 100\% \quad (4)$$

Here, m_0 and m_1 are the mass of the sample before and after drying, respectively.

According to the Curie equation (5), the magnitude of thermal equilibrium magnetization vector was inversely proportional to the temperature,

$$M = \frac{N\gamma^2 h^2 I(I+1)H_0}{3kT} \quad (5)$$

Here, M is magnetization, N is spin density, γ is gyromagnetic ratio, h is Planck constant divided by 2π, I is the spin quantum number, H_0 is magnetic field strength, k is Boltzmann constant, and T is the absolute temperature. In order to eliminate the influence of temperature during experiments, the amplitudes measured at different temperatures were multiplied by the factor T_x/T_0, where T_x is the actual temperature and T_0 is the reference temperature. In this experiment, the room temperature was selected as T_0 (Telkki *et al.* 2013).

The total content of bound water when the cell wall was saturated is obtained from Eq. 6.

$$M_b = MC \cdot \frac{S_{-3°C}}{S_{normal}} \quad (6)$$

Here, MC is determined gravimetrically, $S_{-3℃}$ is integral of moisture peaks at -3 °C, and S_{normal} is integral of moisture peaks at room temperature. The unfrozen bound water amount at other temperatures could be calculated using Eq. 7,

$$M_{tx} = MC \cdot \frac{S_{tx}}{S_{normal}} \quad (7)$$

Here, S_{tx} is integral of moisture peaks at freezing the temperature of T_x.

The diameter distribution (DD) is determined by the intensity corresponding to the pore size with a certain melting temperature given by the Gibbs-Thomson equation according to Table 1. The diameter distribution proportion within a certain range could be determined by Eq. 8,

$$DD = \frac{M_{D\alpha} - M_{D_\beta}}{M_b} \quad (8)$$

Here, $M_{D\alpha}$ and $M_{D\beta}$ are the amount of unfrozen bound water in the pore which diameter is Dx, respectively.

The slices for anatomical structure analysis were made by microtome (REM 170, YAMATO Corporation, Japan) and dyed with safranine. The Lecia DM1000 (Lecia Corporation, Germany) optical microscope was used to analyze the anatomical structure.

RESULTS AND DISCUSSION

Relaxation Time Distributions at Different Temperatures

T_2 relaxation time distributions of 5 species at -40 °C to room temperature and anatomical structure are presented in Fig.1. Above the melting point (24 °C), the T_2 distributions of softwood (*Pinus sylvestris* and *Cunninghamia lanceolata*) contain three peaks. The T_2 times of the three peaks were several ms, dozens of ms, and hundreds of ms. According to previous research, the shortest T_2 peaks were interpreted to have arisen from bound water, while the other peaks arose from free water. The T_2 relaxation time of water in porous media could be considered approximately proportional to pore diameter. The principal structure of softwoods is the longitudinal tracheids, with approximately 92% of volumetric composition (Almedia *et al.* 2008). Because of the wood physiology, tracheids formed during the summer (latewood) have lumens much smaller than those formed during spring (earlywood). The two peaks of free water could be attributed to the differences in diameters of the tracheids. For hardwoods, the T_2 distributions of poplar contained three peaks, while ash and balsa wood showed four peaks under room temperature. The T_2 peaks of the poplar that belong to diffuse-porous wood could be considered as arising from bound water in cell wall and free water in fiber and vessel. However, because of the ash belonging to ring-porous wood, there were significant changes to the diameter of the vessel in the growth ring, which led to three typical scale cavities. The T_2 distributions of balsa wood also show four peaks. Although balsa wood is also a kind of diffuse-porous wood, the T_2 distributions show four peaks that are different from poplar. Balsa wood is a special species with low-density ranges from roughly 50 to 380 kgm^{-3} (Borrega *et al.* 2015). Distinguished from other species, there are plenty of axial parenchyma whose diameters are significantly larger than fibers; therefore, the T_2 distributions of balsa wood also show four peaks. They could be considered to be arising from moisture in cell wall, wood fibers, axial parenchymas, and vessels from the left to the right part of the T_2 distributions.

Below the melting point of bulk water, the free water is frozen with enough time so that the remaining moisture signals arise exclusively from bound water. The T_2 distributions show a single shorter time peak under a different freezing temperature.

Bound Water Content of Swollen Cell Wall under Different Freezing Treatments

The integrals of moisture at different freezing temperatures are shown in Table 2. According to Eq. 4, the moisture content of water-saturated samples are as follows: 283% (pine), 290% (Chinese fir), 218% (poplar), 119% (ash), and 780% (balsa wood), and the total bound water contents of swollen cell walls were: 39.9%, 38.2%, 38.3%, 34.6%, and 48.1%, respectively. The bound water content determined by the NMR method was approximately 40%. For balsa wood the values were even as high as 50%; such results are significantly higher than the fiber saturation point that is presumed to be 30%. Actually, the values of FSP obtained by different methods varied in the range of 13% to 70%. The analysis of the methods presented shows that the determined FSP value could be strongly influenced by the method used (Babiak and Kúdela 1995). Typically, the FSP measured by extrapolation is about 30%. This method is based upon conditioning wood at a chosen relative humidity and the measurement of the moisture content and physical or mechanical properties of wood. Then, the FSP will be determined by extrapolating the

measured sorption isotherm to the relative humidity of 100%. However, the FSP determined by extrapolation may underestimate the saturated content of bound water. Methods including solute exclusion, porous plate, centrifugal dehydration, DSC, *etc*., which are all supposed to measure the bound water content of swollen cell wall, may result in FSP values above 40%. It was found that the specimens that were conditioned at 100% relative humidity would further swell when soaked in water; therefore, it is reasonable to believe that the limitation of bound water would be underestimated just by isothermal adsorption even in 100% relative humidity air (Babiak and Kúdela 1995). To solve this problem some researchers suggested dividing the bound water saturation limit into two parts: hygroscopicity limit (HL) and cell wall saturation limit (CWS) (Babiak and Kúdela 1995). HL is the moisture content limit adsorbing in water vapor, and the latter is acquired by soaking in water. CWS should be greater than HL. In this experiment, all the samples were boiled to saturate with distilled water before NMR scanning. The total bound water content could be corresponding to CWS.

The bound water values of softwoods in this experiment were close to the values detected by solute exclusion [35% to 40% Walker (2006); 38% to 40% Hill (2006)] and NMR method [35% to 45% Telkki *et al.* (2013)]. The values of poplar were similar to the results by the porous plate method [40% Cloutier *et al.* (1991, 1995)]. The values of ash were similar to the results by the DSC method [35% Zauer *et al.* (2014)]. The bound water content of balsa wood was 48.1%, which is significantly higher than other species. Feist and Tarkow (1967) tested the bound water content of balsa wood by the solute exclusion method; they obtained an even higher bound water content of 52%.

From the results above, an obvious relationship was found between the cell wall saturation limit and the basic density of different species. With the decrease of basic density, the cell wall saturation limit increases. The bound water content of high density species (*Fraxinus excelsior* L.) was about 35%, the medium density species (softwoods and poplar) was approximate 40%, and the lowest density (*Ochroma lagopus*) could be as high as 50%. The experimental result was consistent with the hypothesis that with a decrease of basic density, more bound water could be contained in cell wall (Feist and Tarkow 1967; Walker 2006). It is suggested that with decreasing basic density, the thickness of cell walls decreases and the cell walls display less resistance to swelling; the bound water content that corresponds to the fiber point represents a balance between the swelling of cell walls and resistance to the mechanical rigidity (Feist and Tarkow 1967; Walker 2006).

The top time of T_2 distribution measured below the bulk melting point decreased with the freezing treatment temperature. According to the Gibbs-Thomson equation, it is evident that with decreasing pore diameter, the melting point depression increased. With decreasing temperatures, the water in the pores that are larger than those determined at the critical temperature will be frozen. The water in the pores that are smaller than those determined at the critical temperature will still be liquid. However, the NMR signal was given because of the relatively smaller pores; therefore, the T_2 top time decreased. In addition, the lower the temperature, the shorter the relaxation time. When the experiment temperature was -40 °C, which is far below the ordinary melting point of bulk water, there was still a NMR signal of liquid water.

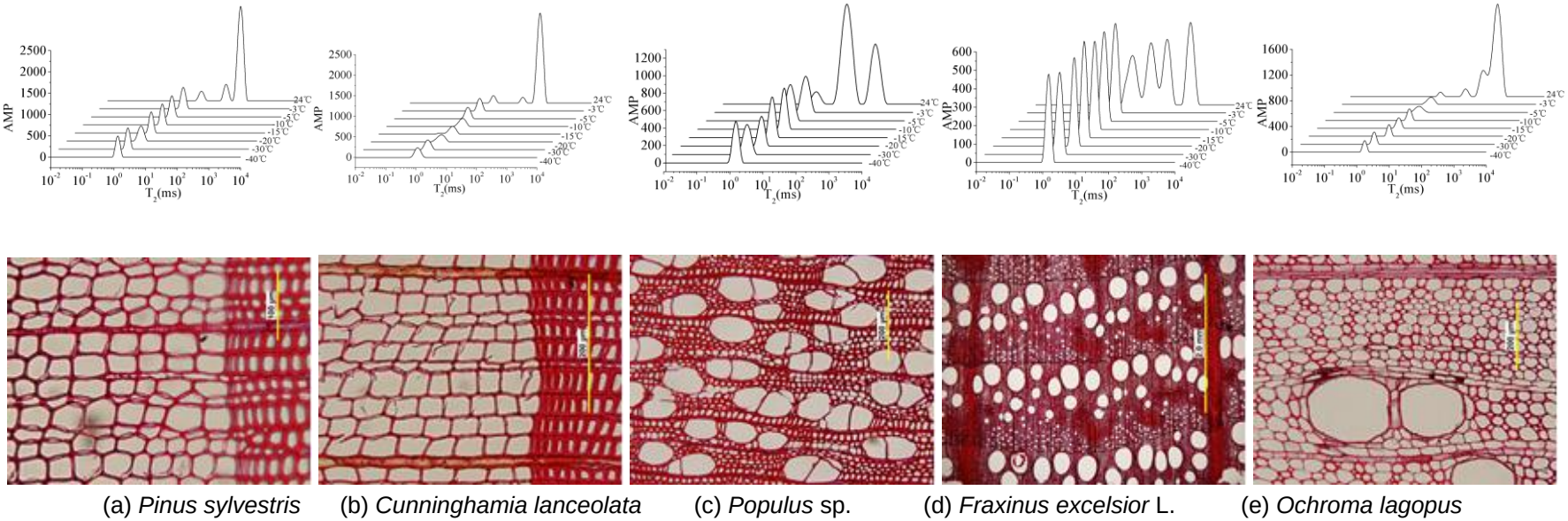

(a) *Pinus sylvestris* (b) *Cunninghamia lanceolata* (c) *Populus* sp. (d) *Fraxinus excelsior* L. (e) *Ochroma lagopus*

Fig. 1. The T_2 distributions at variable temperatures and the anatomical structure of various species

Table 2. The Top Time, Peak Area (Integrals of Amplitude), and Moisture Content from T_2 Distributions of Samples at Different Temperatures

T (°C)	*D* (nm)	*Pinus sylvestris*			*Cunninghamia lanceolata*			*Populus* sp.			*Fraxinus excelsior* L.			*Ochroma lagopus*		
		TT*	PA*	MC	TT	PA	MC	TT	PA	MC	TT	PA	MC	TT	PA	MC
+24	-	5.75	30537	283%	5.87	19602	290%	6.36	23944	218%	5.84	19048	119%	6.75	26335	780%
-3	13.80	4.57	4305	39.9%	4.32	2582	38.2%	5.54	4212	38.3%	4.67	5540	34.6%	6.16	1624	48.1%
-5	8.52	3.48	4230	39.2%	3.70	2546	37.7%	4.50	4046	36.8%	3.87	5483	34.2%	4.95	1582	46.7%
-10	4.56	3.21	4035	37.9%	3.26	2503	37.0%	4.19	3959	36.0%	3.54	5065	31.6%	4.06	1479	43.8%
-15	3.24	2.64	3625	33.9%	2.81	2442	36.1%	3.18	3876	35.2%	3.08	4867	30.4%	3.38	1442	42.7%
-20	2.58	2.17	3570	33.1%	2.13	2251	33.3%	2.77	3691	33.6%	2.80	4359	27.2%	3.08	1348	39.9%
-30	1.92	1.53	3476	32.2%	1.34	2120	31.3%	1.83	3352	30.5%	1.85	4242	26.5%	1.94	1255	37.2%
-40	1.59	1.32	3336	30.9%	1.11	1935	28.6%	1.48	2952	26.8%	1.54	4032	25.2%	1.77	1226	36.3%

*TT: Top Time of the peak, PA: Peak Area

Table 3. Pore Size Distributions of the Swollen Cell Wall

*DD** (nm)	*Pinus sylvestris*	*Cunninghamia lanceolata*	*Populus* sp.	*Fraxinus excelsior* L.	*Ochroma lagopus*
4.56~13.80	5.1%	3.1%	6.0%	8.8%	8.9%
2.58~4.56	12.0%	9.7%	6.3%	12.7%	8.1%
1.59~2.58	5.6%	12.3%	15.8%	5.8%	7.5%
<1.59	77.4%	74.9%	70.0%	72.8%	75.5%

**DD*: Diameter Distribution

The moisture content of bound water that had not been frozen was: 30.9%, 28.6%, 26.8%, 25.2%, and 36.3% for pine, Chinese fir, poplar, ash, and balsa wood, respectively. This accounted for 77.4%, 74.9%, 70.0%, 72.8%, and 75.5% of the total amount of bound water obtained by the peak integrals of -3 °C, respectively. The results of softwoods were similar to the experiment measured by time domain reflection technology. In the experiment of Sparks *et al.* (2000), there was more than 25% water unfrozen when temperature was below -15 °C. The moisture in wood was completely frozen when the temperature was below -75 °C. The minimum operating temperature of the NMR system for this experiment is -40 °C, therefore, the relaxation distributions of moisture in wood for lower temperature need to be further studied.

Pore Size Distribution of Swollen Cell Wall

The pore size distributions of swollen cell walls are shown in Table 3. The proportion of pore diameter smaller than 1.59 nm was 77.4%, 74.9%, 70.0%, 72.8%, and 75.5% for pine, Chinese fir, poplar, ash, and balsa wood, respectively. The proportion of pore diameter between 1.59 to 2.58 nm was 5.6%, 12.3%, 15.8%, 5.8%, and 7.5%. The proportion of pore diameter greater than 4.56 nm was 5.1%, 3.1%, 6.0%, 8.8%, and 8.9%, which indicates that the majority of pores in swollen cell walls are relatively minute. This corresponds to the results by the solute exclusion method. Stone and Scallan (1968) used a series of smaller polymer probes that were calculated to have "equivalent spherical diameters" in the range of 0.8 to 56 nm. This was done in order to investigate the pore size and pore volume within the swollen cell wall of softwoods. It was indicated that the pore size distribution of the cell walls was not homogeneous. The moisture in the pore larger than 5 nm was no more than 10% of the total quantity of bound water. The moisture in the pore smaller than 1 nm was not less than 50%. The proportion of pore diameter below 2 nm was about 70%. According to the results of the present experiment, the pore volume below 1.59 nm and 1.92 nm was about 70% and 80%, which is higher than the solute exclusion method results. The differences between the results may be due to the experimental principles. As mentioned in the introduction, the principle of the solute exclusion method is that probe molecules enter the pores larger than them and replace the water and the pore volume of the wood is measured by the decrease in concentration of the probe solution. Therefore, the volume relates to the size of polymer probes. In Stone and Scallan's experiment, the probe could not diffuse into the pores smaller than 0.8 nm, which means the volume may be underestimated (Hill 2006; Walker 2006). Meanwhile, the actual size of polymer probes is relatively idealized. First, the diameter of the polymer is determined by dividing molar volume to Avogadro constant. But, the molecular weight of the polymer used in the experiment always changes in a certain range. Second, the shape of the polymer is supposed to be spherical, which in reality, is a chain structure. From the results of solute exclusion, there were only approximately 5% of pores larger than 3.6 nm, which is similar to the results of the present experiment. The proportion of pores above 4 nm is no more than 10%, which corresponds to most studies that report a maximum size for swollen cell wall micropores in the region of 2 to 4 nm (Stone and Scallan 1968; Walker 2006; Hill 2006).

Telkki *et al.* (2013) used NMR to determine the FSP of softwoods. In his experiment the lowest freezing temperature was -20 °C, in which about 10% of bound water was frozen. According to Gibbs-Thomson, the corresponding pores' diameter is

about 2 nm; meaning that 90% of bound water is in the pores that are smaller than 2 nm, which is similar to this experiment (85%).

The pore distributions are different depending on the species; this should be attributed to the differences of the microstructure between different species. Donaldson (2007) found that there were differences between microfibrils for different species; this may influence the sizes of pores existing between the microfibrils.

CONCLUSIONS

1. NMR cryoporometry could be used to determine the bound water content and pore size distributions of the swollen cell walls of wood. The basis of this method is to measure the moisture NMR signal changes under different freezing temperatures according to Gibbs-Thomson effect.
2. By comparing the differences between the T_2 relaxation distributions above and below the melting, the total bound water content of different species were determined: *Pinus sylvestris* 39.9%, *Cunninghamia lanceolata* 38.2%, *Populus* sp. 38.3%, *Fraxinus excelsior* L. 34.6%, *Ochroma lagopus* 48.1%. The results were obviously higher than the FSP (appr. 30%), which were measured by the extrapolation method. However, they were similar to the results by solute exclusion and pressure plate methods, which can determine the bound water content of saturated wood samples.
3. The swollen bound water content of different species was consistent with the hypothesis that with the decrease of basic density, the more bound water could be contained.
4. The experiment results indicated that the proportion of the pore diameter smaller than 1.59 nm was higher than 70%, and that the proportion of the pore diameter larger than 4 nm was no more than 10%, which is similar to the results of the solute exclusion method.

ACKNOWLEDGMENTS

The authors are grateful for the support from the National Science and Technology Support Plan of China (NO. 2012BAD24B01) and Jiangsu Province Ordinary University Graduate Student Scientific Research Innovation Project (NO. CXZZ13_0543).

REFERENCES CITED

Aksnes, D. W., and Kimtys, L. (2004). "1H and 2H NMR studies of benzene confined in porous solids: Melting point depression and pore size distribution," *Solid State Nucl. Mag.* 25(1-3), 146-152. DOI: 10.1016/j.ssnmr.2003.03.001

Almeida, G., Gagné S., and Hemándes, R. E. (2007). "A NMR study of water distribution in hardwoods at several equilibrium moisture contents," *Wood Sci. Technol.* 41(4), 293-307. DOI: 10.1007/s00226-006-0116-3

Almeida, G., Leclerc, S., and Perre, P. (2008). "NMR imaging of fluid pathways during drainage of softwood in a pressure membrane chamber," *Int. J. Multiphas. Flow* 34(3), 312-32. DOI: 10.1016/j.ijmultiphaseflow.2007.10.009

Araujo, C. D., MacKay, A. L., Hailey, J. R. T., and Whittall, K. P. (1992). "Proton magnetic resonance techniques for characterization of water in wood: application to white spruce," *Wood Sci. Technol.* 26(2), 101-113.

Babiak, M., and Kúdela, J. (1995). "A contribution to the definition of the fiber saturation point," *Wood Sci. Technol.* 29(3), 217-226.

Bolton, A. J., Dinwoodie, J. M., and Davies, D. A. (1988). "The validity of the use of SEM/EDXA as a tool for the detection of UF resin penetration into wood cell walls of particleboard," *Wood Sci. Technol*. 22(4), 345-356.

Borrega, M., Ahvenainen, P., Serimaa, R., and Gibson, L. (2015). "Composition and structure of balsa (*Ochroma lagopus*) wood," *Wood Sci. Technol.* 49(2), 403-420. DOI: 10.1007/s00226-015-0700-5

Cavallaro, G., Donato, D. I., Lazzara, G., and Milioto, S. (2013). "Determining the selective impregnation of waterlogged archaeological woods with poly(ethylene) glycols mixtures by differential scanning calorimetry," *J. Therm. Anal. Calorim*. 111(2), 1449-1455. DOI: 10.1007/s10973-012-2528-7

Cloutier, A., and Fortin, Y. (1991). "Moisture content-water potential relationship of wood from saturated to dry conditions," *Wood Sci. Technol.* 25(4), 263-280.

Cloutier, A., Tremblay, C., and Fortin, Y. (1995). "Effect of specimen structural orientation on the moisture content-water potential relationship of wood," *Wood Sci. Technol.* 29(4), 235-242.

Donaldson, L. (2007). "Cellulose microfibril aggregates and their size variation with cell wall type," *Wood Sci. Technol*. 41(5), 443-460. DOI: 10.1007/s00226-006-0121-6

Feist, W. C., and Tarkow, H. (1967). "A new procedure for measuring fiber saturation points," *For Prod. J*. 17(10), 65-68.

Furuno, T., Imamura, Y., and Kajita, H. (2004). "The modification of wood by treatment with low molecular weight phenol-formaldehyde resin: A properties enhancement with neutralized phenolic-resin and resin penetration into wood cell walls," *Wood Sci. Technol.* 37(5), 349-361. DOI: 10.1007/s00226-003-0176-6

Gabrielli, C. P., and Kamke, F. A. (2010). "Phenol-formaldehyde impregnation of densified wood for improved dimensional stability," *Wood Sci. Technol.* 44(1), 95-104. DOI: 10.1007/s00226-009-0253-6

Gierling, N., Hansmann, C., Röder, T., Sixta, H., Gindl, W., and Wimmer, R. (2005). "Comparison of UV and confocal Raman microscopy to measure the melamine-formaldehyde resin content within cell walls of impregnated spruce wood," *Holzforschung* 59(2), 210-213. DOI: 10.1515/HF.2005.033

Gindl, W., Zargar-Yaghubi, F., and Wimmer, R. (2003). "Impregnation of softwood cell walls with melamine- formaldehyde resin," *Bioresour. Technol*. 87(3), 325-330. DOI: 10.1016/S0960-8524(02)00233-X

Gouze, B., Cambedouzou, J., Maynadie, S. P., and Rebiscoul, D. (2014). "How hexagonal mesoporous silica evolves in water on short and long term: Role of pore

size and silica wall porosity," *Micropor. Mesopor. Mat.* 183, 168-176. DOI: 10.1016/j.micromeso.2013.08.041

Hartley, I. D., Kamke, F. A., and Peemoeller, H. (1994). "Absolute moisture content determination of aspen wood below the fiber saturation point using pulsed NMR," *Holzforschung* 48(6), 474-479. DOI: 10.1515/hfsg.1994.48.6.474

Hassan, J. (2012). "Pore size distribution calculation from 1H NMR signal and N_2 adsorption-desorption techniques," *Physica B.* 407(18), 3797-3801. DOI: 10.1016/j.physb.2012.05.063

Hill, C. A. S. (2006). *Wood Modification: Chemical, Thermal and Other Processes*, John Wiley & Sons, Hoboken, NJ.

Hiroshi, M., Makoto, K., Evans, P. D. (2009). "Microdistribution of copper-carbonate and iron oxide nanoparticles in treated wood," *J. Nanopart. Res.* 11, 1087-1098. DOI: 10.1007/s11051-008-9512-y

Hoffmann, P. (1990). "The stabilization of waterlogged softwoods with polyethylene glycol (PEG). Four species from China and Korea," *Holzforschung* 44(2), 87-93. DOI: 10.1515/hfsg.1990.44.2.87

Jeremic, D., Cooper, P., and Heyd, D. (2007). "PEG bulking of wood cell walls as affected by moisture content and nature of solvent," *Wood Sci. Technol.* 41(7), 597-606. DOI: 10.1007/s00226-006-0120-7

Jeremic, D., and Cooper, P. (2009). "PEG quantification and examination of molecular weight distribution in wood cell walls," *Wood Sci. Technol.* 43(3-4), 317-329. DOI: 10.1007/s00226-008-0233-2

Kekkonen, P. M., Ylisassi, A., and Telkki, V. V. (2014). "Absorption of water in thermally modified pine wood as studied by nuclear magnetic resonance," *J. Pyys. Chem. C.* 118(4), 2146-2153. DOI: 10.1021/jp411199r

Labbé, N., DeJéso, B., Lartigue, J. C., Daudé, G., Pétraud, M., and Ratier, M. (2002). "Moisture content and extractive materials in maritime pine wood by low field 1H NMR," *Holzforschung* 56(1), 25-31. DOI: 10.1515/HF.2002.005

Mattos, B. D., Lourençon, T. V., Serrano, L., Labidi, J., and Gatto, D. A. (2015). "Chemical modification of fast-growing eucalyptus wood," *Wood Sci. Technol*. 49(2), 273-288. DOI: 10.1007/s00226-014-0690-8

Maunu, S. L. (2002). "NMR studies of wood and wood products," *Prog. Nucl. Magn. Reson. Spectrosc.* 40(2), 151-174. DOI: 10.1016/S0079-6565(01)00041-3

Menon, R. S., MacKay, A. L., Hailey, J. R. T., Bloom, M., Burgess, A. E., and Swanson, J. S. (1987). "An NMR determination of the physiological water distribution in wood during drying," *J. Appl. Polym.* Sci. 33(4), 1141-1155. DOI: 10.1002/app.1987.070330408

Östlund, Å., Köhnke, T., Nordstierna, L., and Nydén, M. (2010). "NMR cryoporometry to study the fiber wall structure and the effect of drying," *Cellulose*. 17(2), 321-361. DOI:10.1007/s10570-009-9383-0

Park, S., Venditti, R. A., Jameel, H., and Pawlak, J. J. (2006). "Changes in pore size distribution during the drying of cellulose fibers as measured by differential scanning calorimetry," *Carbohydr. Polym.* 66(1), 97-103. DOI: 10.1016/j.carbpol.2006.02.026

Provencher, S. W. (1982a). "A constrained regularization method for inverting data represented by linear algebraic or integral equations," *Comput. Phys. Commun.* 27(3), 213-227. DOI: 10.1016/0010-4655(82)90173-4

Provencher, S. W. (1982b). "CONTIN: A general purpose constrained regularization program for inverting noisy linear algebraic and integral equations," *Comput. Phys. Commun.* 27(3), 229-242. DOI: 10.1016/0010-4655(82)90174-6

Riggin, M. T., Sharp, A. R., and Kaiser, R. (1979). "Transverse NMR relaxation of water in wood," *J. Appl. Polym. Sci.* 23(11), 3147-3154. DOI: 10.1002/app.1979.070231101

Sharp, A. R., Riggin, M. T., Kaiser, R., and Schneider, M. H. (1978). "Determination of moisture content of wood by pulsed nuclear magnetic resonance," *Wood Fiber Sci*. 10(2), 74-81.

Simpson, L., and Barton, A. F. M. (1991). "Determination of the fibre saturation point in the whole wood using differential scanning calorimetry," *Wood Sci. Technol*. 25(4), 301-308.

Smith, L. A., and Côté, W. A. (1971). "Studies of penetration of phenol-formaldehyde resin into wood cell walls with the SEM and energy-dispersive X-ray analyzer," *Wood Fiber Sci.* 3(1), 56-57.

Smith, L. A., and Côté, W. A. (1972). "Resin penetration into wood cell walls." *J. Paint Technol.* 44(564), 71.

Sparks, J. P., Campbell, G. S., and Black, R. A. (2000). "Liquid water content of wood tissue at temperatures below 0 degrees," *Can. J. Forest Res.* 30(4), 624-630. DOI: 10.1139/cjfr-30-4-624

Stone, J. E., and Scallan, A. M. (1968). "Structural model for the cell wall of water-swollen wood pulp fibers based on their accessibility to macromolecules," *Cellulose Chem. Technol.* 2(1), 343-358.

Telkki, V. V., Yliniemi, M., and Jokisaari, J. (2013). "Moisture in softwoods: Fiber saturation point, hydroxyl site content, and the amount of micropores as determined from NMR relaxation time distributions," *Holzforschung* 67(3), 291-300. DOI: 10.1515/hf-2012-0057

Thygesen, L. G., and Elder, T. (2008). "Moisture in untreated, acetylated and furfurylated Norway spruce studied during drying using time domain NMR," *Wood Fiber Sci.* 40(3), 309-320.

Tian, H. H., Wei, C. F., Wei, H. Z., Yan, R. T., and Chen, P. (2014). "An NMR-based analysis of soil-water characteristics," *Appl. Magn. Reson*. 45(1), 49-61. DOI: 10.1007/s00723-013-0496-0

Wacker, J. P. (2010). "Use of wood in buildings and bridges," in: *Wood Handbook: Wood as an Engineering Material, General Technical Report FPL-GTR-190*, U.S. Department of Agriculture, Forest Service, Forest Products Laboratory, Madison, WI.

Walker, J. C. F. (2006). "Chapter 3: Water in wood," in *Primary Wood Processing Principles and Practice, Second Edition*, 69-94 Springer (ed.) University of Canterbury, Christchurch, New Zealand.

Wallström, L., and Lindberg, K. A. H. (1999). "Measurement of cell wall penetration in wood of water-based chemicals using SEM/EDS and STEM/EDS technique," *Wood Sci. Technol.* 33(2), 111-122.

Westphal, H., Surholt, I., Kiesl, C., Thern, H. F., and Kruspe, T. (2005). "NMR measurements in carbonate rocks: Problems and an approach to a solution," *Pure Appl. Geophys.* 162(3), 549-570. DOI: 10.1007/s00024-004-2621-3

Xie, Y., Qiliang, F., Qingwen, W., Zefang, X., and Holger, M. (2013). "Effects of chemical modification on the mechanical properties of wood," *Eur. J. Wood Prod.* 71(4), 401-416. DOI: 10.1007/s00107-013-0693-4

Zauer, M., Kretzschmar, J., Großmann, L., Pfriem, A., and Wangenführ, A. (2004). "Analysis of the pore-size distribution and fiber saturation point of native and thermally modified wood using differential scanning calorimetry," *Wood Sci. Technol.* 48(1), 177-193. DOI: 10.1007/s00226-013-0597-9

Article submitted: June 4, 2015; Peer review completed: August 24, 2015; Revised version received: August 31, 2015; Accepted: September 1, 2015; Published: October 27, 2015.
DOI: 10.15376/biores.10.4.8208-8224